ISSN 1936-878X/09/$36.00
PUBLISHED BY ELSEVIER INC.
DOI:10.1016/j.jcmg.2009.05.014

Assessment of Myocardial Edema by Computed Tomography in Myocardial Infarction

Andreas H. Mahnken, MD, MBA,*† Philipp Bruners, MD,*† Christoph M. Bornikoel, MD,* Nils Krämer, MD,* Rolf W. Guenther, MD*

Aachen, Germany

OBJECTIVES The aim of this study was to analyze whether cardiac computed tomography (CT) permits the assessment of myocardial edema in acute myocardial infarction (MI).

BACKGROUND Several studies proved the value of detecting myocardial edema from T2-weighted cardiac magnetic resonance (CMR) for differentiating acute from chronic MI. Computed tomography is suited for depicting MI, but there are no data on CT imaging of myocardial edema. We hypothesized that areas of reduced attenuation in acute MI may correspond to edema.

METHODS In 7 pigs (55.2 ± 7.3 kg), acute MI was induced using a closed chest model. Animals underwent unenhanced arterial and late-phase dual source computed tomography (DSCT) followed by T2-weighted and delayed contrast-enhanced CMR. Animals were sacrificed, and the excised hearts were stained with 2,3,5-triphenyltetrazolin chloride (TTC). Size of MI, contrast-to-noise ratio, and percent signal difference were compared among the different imaging techniques with concordance-correlation coefficients (ρ_c), Bland-Altman plots, and analysis of variance for repeated measures.

RESULTS Infarction was transmural on all slices. On unenhanced, arterial, and late-phase DSCT, mean sizes of MI were 27.2 ± 8.5%, 20.1 ± 6.9%, and 23.1 ± 8.2%, respectively. Corresponding values on T2-weighted and delayed enhanced CMR were 28.5 ± 7.8% and 22.2 ± 7.7%. Size of MI on TTC staining was 22.6 ± 7.8%. Best agreement was observed when comparing late-phase CT (ρ_c = 0.9356) and delayed enhanced CMR (ρ_c = 0.9248) with TTC staining. There was substantial agreement between unenhanced DSCT and T2-weighted CMR (ρ_c = 0.8629). Unenhanced DSCT presented with the lowest percent signal difference (46.0 ± 18.3) and the lowest contrast-to-noise ratio (4.7 ± 2.0) between infarcted and healthy myocardium.

CONCLUSIONS Unenhanced DSCT permits the detection of myocardial edema in large acute MI. Further studies including smaller MI in different coronary artery territories and techniques for improving the contrast-to-noise ratio are needed. (J Am Coll Cardiol Img 2009;2:1167–74) © 2009 by the American College of Cardiology Foundation

From the Departments of *Diagnostic Radiology and †Applied Medical Engineering, RWTH Aachen University, Aachen, Germany.

Manuscript received May 5, 2009; accepted May 7, 2009.

Differentiating acute from chronic myocardial infarction (MI) and detecting the myocardium at risk, which may benefit from reperfusion therapy after acute MI, are major demands for decision making. Several studies proved the value of T2-weighted cardiac magnetic resonance (CMR) for differentiating acute from chronic MI (1,2). Whereas acute MI is accompanied by myocardial edema, chronic MI is not. Detection of myocardial edema may also help to identify the peri-infarction zone, which is considered the area at risk (3). The latter has been proposed to correspond to the hyperintense area on T2-weighted CMR images after subtracting areas of delayed contrast enhancement (4). Consequently, this technique is increasingly used in clinical routine practice.

With the introduction of cardiac computed tomography (CT) in clinical routine practice, previous efforts for assessing MI were revived, and several studies proved the current cardiac CT technique reliable for detecting MI (5–8). For this purpose, a variety of CT techniques were evaluated, including CT imaging of myocardial perfusion (9), arterial phase perfusion deficit (10,11), and delayed myocardial contrast enhancement. Assessment of wall motion abnormalities and wall thinning was proved feasible, too. However, there are no data on in vivo CT imaging of myocardial edema.

From early studies on CT imaging of MI, it is known that acute MI may present as areas of reduced CT values on unenhanced CT (12,13). Theoretically, increased water content should result in a decrease of the CT value when compared with healthy myocardium. Therefore, we hypothesized that these areas of reduced attenuation values may correspond to myocardial edema rather than to MI. Consequently, the aim of this study was to analyze whether cardiac CT permits the assessment of myocardial edema in acute MI.

ABBREVIATIONS AND ACRONYMS

CMR = cardiac magnetic resonance
CNR = contrast-to-noise ratio
CT = computed tomography
DSCT = dual-source computed tomography
ECG = electrocardiogram
LV = left ventricular
MI = myocardial infarction
SNR = signal-to-noise ratio
TTC = 2,3,5-triphenyltetrazolin chloride

METHODS

Animal model. Seven domestic pigs weighing 55.2 ± 7.3 kg were included in this study after approval from the State Committee on Animal Affairs. After intramuscular pre-medication with 0.5-ml atropine 1% (Atropinum Sulfuricum Solution 1%, WDT, Garbsen, Germany), 0.2 mg/kg azaperone (Stresnil, Janssen-Cilag, Neuss, Germany), and 5-mg/kg ketamine (Ketamin 10%, Ceva, Düsseldorf, Germany), anesthesia was induced by intravenous injection of diluted pentobarbital (Narcoren, Merial, Hallbergmoos, Germany) through an 18-G venous access line placed in an ear vein. All animals were orotracheally intubated and mechanically ventilated with an oxygen and air mixture containing 1.0 Vol% Isoflurane (Abbott, Baar, Switzerland) at a respiratory rate of 15 min^{-1}. For pain management, 0.01-mg/kg buprenorphine (Temgesic, Essex Pharma, Munich, Germany) was administered intramuscularly.

Acute reperfused MI was induced using a closed chest model. A 7-F guiding catheter (Vista Brite Tip, Cordis, Miami Lakes, Florida) was positioned at the origin of the left coronary artery through the right femoral approach. After a coronary angiogram was obtained for visualizing the left coronary anatomy, the mid section of the left circumflex artery was occluded for 60 min by inflation of an individually sized 2.5- to 3-mm balloon catheter (Hayate, Terumo, Tokyo, Japan). Complete vessel occlusion and reperfusion were proven by repeated coronary angiograms. Continuous electrocardiography (ECG) monitoring was available, and in case of left ventricular (LV) fibrillation, direct current defibrillation was performed.

Imaging procedures. Sixty minutes after reperfusion, all animals underwent CMR using a clinical 1.5-T whole body MR scanner equipped with a dedicated 5-element cardiac synergy coil (Gyroscan Intera, Philips Medical Systems, Best, the Netherlands). Animals were positioned supine, and ventilation was suspended in end-expiration during image acquisition. First, a T2-weighted ECG-triggered, inversion-recovery, black-blood, turbo spin-echo sequence was used. Sequence parameters included an echo time of 100 ms with a repetition time of 2 heart beats, turbo spin-echo factor of 33, slice thickness of 6 mm without interslice gap, field of view of 370 × 370 mm^2, and a 512 × 512 matrix reconstructed to 0.72 × 0.72 mm^2 in-plane resolution. Starting 10 min after intravenous injection of 0.2-mmol/kg body weight gadolinium-diethylenetriaminepentaacetic acid (Gd-DTPA [Magnevist, Bayer-Schering, Berlin, Germany]), a prospectively ECG-gated T1-weighted gradient echo sequence with an inversion pre-pulse was used to acquire diastolic 6-mm short-axis slices without an interslice gap. Imaging parameters were as follows: TR 2 heartbeats, TE 5.0 ms, flip angle 25°, field of view 380 × 380 mm^2, matrix 256 × 256, and reconstructed voxel size 1.48 × 1.48 × 6 mm^3.

The trigger delay was adjusted per pig to acquire data in mid- to end-diastole, and the inversion time of the pre-pulse varied according to subjective visual judgment from 260 to 285 ms to null the signal of remote myocardium and to achieve optimal image contrast between infarcted and viable myocardium.

For CT imaging, a 64-slice DSCT scanner (SOMATOM Definition, release VA11, Siemens, Forchheim, Germany) was used. The pigs were positioned supine, and all scans were performed in the craniocaudal direction during end-expiratory breath hold. A standardized examination protocol with $2 \times 64 \times 0.6$ mm collimation for both detectors, tube rotation time of 330 ms, and an individually heart rate-adapted pitch ranging from 0.25 to 0.48 was applied for all scans. Tube voltage was 120 kV in both tubes, with a tube current-time product of 380 mAs_{rot}. Tube current modulation was not applied.

First, an unenhanced CT scan was performed. For arterial phase CT, 120-ml iopromide 300 (Ultravist 300, Bayer-Schering Pharma AG, Berlin, Germany) was administered through an 18-G access in an ear vein at a flow rate of 6.2 ml/s followed by a 50-ml saline chaser bolus at the same flow rate. The scan delay was determined using the bolus tracking technique. Data acquisition started 5 s after a threshold of 180 Hounsfield Units (HU) was reached in a region of interest placed in the ascending aorta. Ten minutes after injection of contrast material, a third DSCT scan was performed for assessing delayed contrast enhancement. Depending on the animal's heart rate, the computed tomography dose index ($CTDI_{Vol}$) ranged from 31.40 to 54.61 mGy.

Double-oblique, 6-mm short-axis images without intersection gap were reconstructed from raw data (3D-Recon, Siemens) at 70% of the RR interval. The temporal resolution was 83 ms fixed. A field of view of 150×150 mm^2, a 512×512 reconstruction matrix, and a smooth convolution kernel (B20f) were chosen.

Finally, the animals were sacrificed with an overdose of intravenous pentobarbital, and the heart was excised, rinsed with saline, and immediately sectioned into 6-mm thick short-axis slices using a plastic pattern. After sectioning, the heart slice thickness was manually controlled with a sliding caliper. The slices were stained with 2% 2,3,5-triphenyltetrazolin-chloride (TTC) solution at 37°C for 15 min. Each section was photographed with 600 dpi using a commercially available digital camera.

Data analysis. All slices showing TTC signs of MI were included in the quantitative analysis. On CMR, infarction or edema was defined as being present if the signal intensity of the hyperintense region on T2-weighted or delayed contrast enhanced images was higher than +3 SD above the mean of the remote myocardium.

On arterial and late-phase DSCT, a mean difference of 20 HU between pathologic enhancement and the mean CT value of the remote myocardium was used to separate infarcted from normal myocardium, as described elsewhere (6). For unenhanced DSCT a difference of 12 HU was used to separate ischemically injured myocardium from healthy myocardium. Regions of interest were manually drawn in the visually assessed areas (Image J, version 1.36b, National Institutes of Health, Bethesda, Maryland). The size of MI and edema was calculated as a percentage of LV area for MR, DSCT, and TTC images. The CT values of normal and ischemically injured myocardium as well as the LV cavity were measured from individually adapted regions of interest. The CT image noise was defined as standard deviation measured in the blood pool of the left ventricle; for CMR signal-to-noise ratio (SNR), noise was computed, with noise being defined as the standard deviation measured in the air outside the animal. For all imaging procedures, contrast-to-noise ratios (CNR) as well as percent signal difference (%difference) between ischemically injured and healthy remote myocardium were calculated as follows:

$$CNR = \frac{meanSI_{MI} - meanSI_{remote}}{meanSI_{noise}}$$

$$\%difference = \frac{meanSI_{MI} - meanSI_{remote}}{meanSI_{remote}}$$

Bland-Altman plots and Lin's concordance-correlation coefficients (ρ_c) were computed to assess agreement of edema and MI size between CMR, the different DSCT techniques, and TTC staining. To find statistically significant differences among the different techniques for assessing myocardial edema and MI, 2-way analysis of variance was conducted separately for the size of edema or MI, CNR, and percent signal difference. In case of statistical significance of the global F test, post-hoc *t* tests were computed for comparison between each pair of measurements. A significance level of 5% was assumed. As this was an explorative study, no alpha-adjustment was performed. Analyses were performed using MedCalc version 10.0.2 (MedCalc, Mariakerke, Belgium).

RESULTS

All interventional and imaging procedures were performed successfully. All imaging studies were suited for further analysis. In all, 4 periods of ventricular fibrillation were observed after coronary occlusion (n = 1) or reperfusion (n = 3) that were successfully treated by direct current defibrillation. The mean heart rates during DSCT and CMR were 77.9 ± 14.5 (range 58 to 99) beats/min and 77.6 ± 13.7 (range 59 to 97) beats/min, respectively.

Twenty-nine CT, MR, and TTC sections presented with signs of ischemic injury and MI. Infarction was transmural on all slices. On unenhanced, arterial, and late-phase DSCT, the mean sizes of ischemically injured myocardium were 27.2 ± 8.5%, 20.1 ± 6.9%, and 23.1 ± 8.2%, respectively. Corresponding values on T2-weighted and delayed enhanced CMR were 28.5 ± 7.8% and 22.2 ± 7.7%. On TTC staining, the mean infarct size was 22.6 ± 7.8% (Fig. 1, Table 1). Analysis of variance revealed a significant difference in the size of MI as determined by the different imaging techniques ($p < 0.0001$). Post-hoc *t* tests revealed significant differences except for the comparison of late-phase CT with delayed enhanced CMR ($p = 0.1005$), and each of them with MI size on TTC staining ($p = 0.4208$ and $p = 0.4271$, respectively). Furthermore, no significant differences were found for the comparison of unenhanced DSCT images with T2-weighted CMR ($p = 0.1139$). Lin's concordance-correlation coefficient showed the highest agreement for the comparison of late-phase CT ($\rho_c = 0.9356$) and delayed enhanced CMR ($\rho_c = 0.9248$) with TTC staining (Table 2). There was also a substantial agreement between unenhanced CT and T2-weighted CMR for assessing the size of edema ($\rho_c = 0.8629$). Bland-Altman plots showed a clinically acceptable mean deviation but a potentially relevant bandwidth of the limits of agreement (Fig. 2). There was no systematic error comparing the different techniques.

Attenuation values and SNR for the different DSCT and CMR techniques are summarized in Table 3. Comparing the different imaging techniques, CMR presented with significantly higher CNR when compared with DSCT. The lowest CNR was found for unenhanced DSCT. On post-hoc *t* tests, CNR differed significantly ($p < 0.0001$), except for the comparison of delayed contrast-enhanced and T2-weighted CMR ($p = 0.8146$). The highest percent signal difference between ischemically injured and normal myocardium was observed for delayed enhanced CMR, which was approximately 9-fold higher than for unenhanced DSCT. Except for the comparison of unenhanced

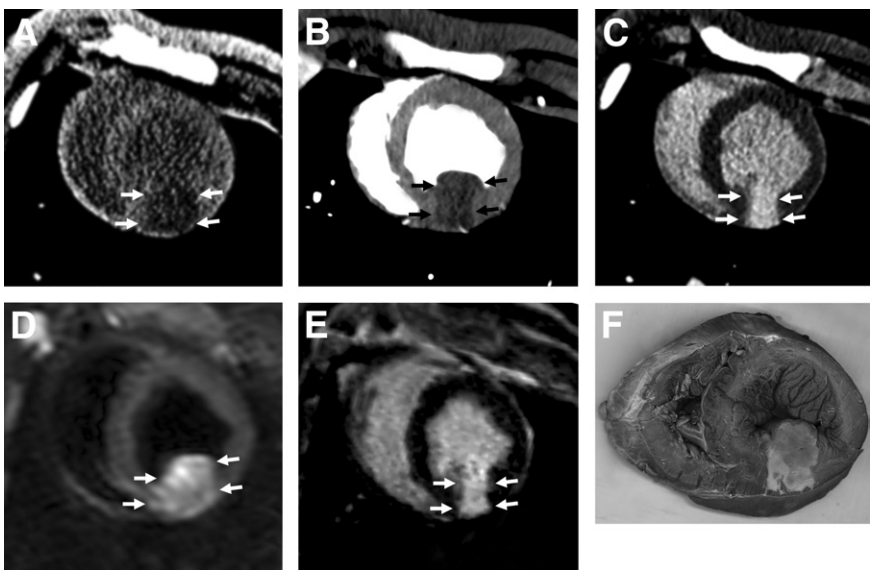

Figure 1. Face-to-Face Comparison of the Different Imaging Techniques

Face-to-face comparison of **(A)** unenhanced, **(B)** arterial, and **(C)** late-phase dual-source computed tomography (CT) with **(D)** T2-weighted and **(E)** delayed enhanced cardiac magnetic resonance (CMR). Size of myocardial infarction on **(C to E)** late-phase CT and CMR **(arrows)** correlates well with **(F)** 2,3,5-triphenyltetrazolin chloride staining. **(A)** Hypodense area of unenhanced CT **(arrows)** correlates best with myocardial edema on **(D)** T2-weighted CMR **(arrows)**.

Table 1. Size and %Difference and CNR for Ischemically Injured Myocardium as Determined With Different DSCT and CMR Techniques in Comparison With Normal Myocardium

	DSCT			CMR			
	Unenhanced	Arterial Phase	Late Phase	T2	DE	TTC	F Test
Size, %	27.2 ± 8.5	20.1 ± 6.9	23.1 ± 8.2	28.5 ± 7.8	22.2 ± 7.7	22.6 ± 7.8	$p < 0.0001$
CNR	4.7 ± 2.0	7.2 ± 2.6	9.8 ± 2.5	49.4 ± 13.0	47.5 ± 13.2	—	$p < 0.0001$
%Difference	46.0 ± 18.3	50.9 ± 23.9	75.4 ± 10.0	98.8 ± 29.0	415.7 ± 305.8	—	$p = 0.0010$

CMR = cardiac magnetic resonance; CNR = contrast-to-noise ratio; DE = delayed enhanced; DSCT = dual-source computed tomography; %Difference = percent signal difference; TTC = 2,3,5-triphenyltetrazolin chloride.

and arterial phase DSCT ($p = 0.5588$), percent signal difference varied significantly ($p < 0.05$) on post-hoc *t* tests.

DISCUSSION

Initially described during the 1970s, CT imaging of MI was never really accepted in clinical routine because of several relevant problems, particularly, limited temporal and spatial resolution (14). Limited temporal resolution caused relevant motion artifacts and, subsequently, early animal studies were performed on ex vivo specimens (13). Insufficient spatial resolution hampered the computation of high-quality multiplanar reformats, resulting in an insufficient assessability of the inferior wall of the left ventricle (15). Some of these problems were overcome with the introduction of electron beam CT. However, limited availability and simultaneous introduction of CMR with its high intrinsic contrast superseded CT imaging of MI. With the introduction of multislice CT and the establishment of CT coronary angiography in clinical routine, efforts were made to advance CT to become a 1-stop-shopping modality for comprehensive imaging of the heart, including the assessment of the global and regional LV function, heart valves, and the myocardium (16).

Only recently, several animal and patient studies proved CT imaging of MI to be a reliable technique (5,6,17,18). From previous studies, it is known that hypodense areas on arterial phase CT imaging as well as hyperdense regions on late-phase CT images obtained 5 to 20 min after contrast material injection, are related to MI (7,14,17,18). However, both imaging techniques have a different substrate. Whereas arterial phase CT depicts a surrogate of perfusion deficits, delayed contrast enhancement on late-phase CT directly shows necrotic myocardium. For arterial as well as late-phase CT, the reported results correlate well with previous studies. After reperfusion, hypodense areas on arterial phase CT are known to typically underestimate the size of MI, when compared with histochemical analysis or delayed contrast enhancement (6,19,20). In this study, there was a substantial agreement between perfusion deficits on arterial phase CT and CMR as well as with TTC staining; nevertheless, arterial phase CT significantly underestimated the size of MI. This underestimation is likely due to pathophysiology. Hypodense areas on arterial phase CT are thought to correspond to perfusion deficits; consequently, they consist of viable and nonviable myocardium. It has been hypothesized that during infarct healing, capillary infiltration from the periphery may not reach the infarct core, resulting in an underestimation of the MI size (20). The excellent agreement between areas of delayed contrast enhancement on late-phase CT and delayed enhanced CMR is in agreement with various studies, indicating the robustness of CT for viability imaging in acute MI (5,6,17,18,21).

None of these techniques shows myocardial edema, which is known to be an important indicator of acute myocardial injury. In this study, it was demonstrated that unenhanced DSCT provides different information about acute ischemic injury when compared with arterial and late-phase CT. Simple theoretical consideration led to the hypothesis that hypodense areas within the LV myocardium correspond to edema, because increased tissue water content should result in a decrease of the CT values when compared with healthy myocardium. This hypothesis is supported by the substantial correlation with the areas of edema on T2-

Table 2. Lin's Concordance-Correlation Coefficients (ρ_c) for Comparison of MI Size Using Different DSCT Techniques With CMR and TTC Staining*

DSCT	T2 CMR	DE CMR	TTC
Unenhanced	$\rho_c = 0.8629$ −1.2 [6.8 to −9.3]	$\rho_c = 0.7511$ 5.0 [12.2 to −2.2]	$\rho_c = 0.7516$ 4.6 [12.6 to −3.5]
Arterial phase	$\rho_c = 0.4788$ −8.4 [0.8 to −17.6]	$\rho_c = 0.8314$ −2.1 [5.2 to −9.5]	$\rho_c = 0.8451$ −2.6 [3.9 to −9.1]
Late phase	$\rho_c = 0.6572$ −5.4 [4.3 to −15.1]	$\rho_c = 0.9336$ 0.9 [6.3 to −4.6]	$\rho_c = 0.9356$ 0.4 [6.0 to −5.1]

*Results from the Bland-Altman approach are given in brackets with mean deviation and upper and lower limits of agreement.
Abbreviations as in Table 1.

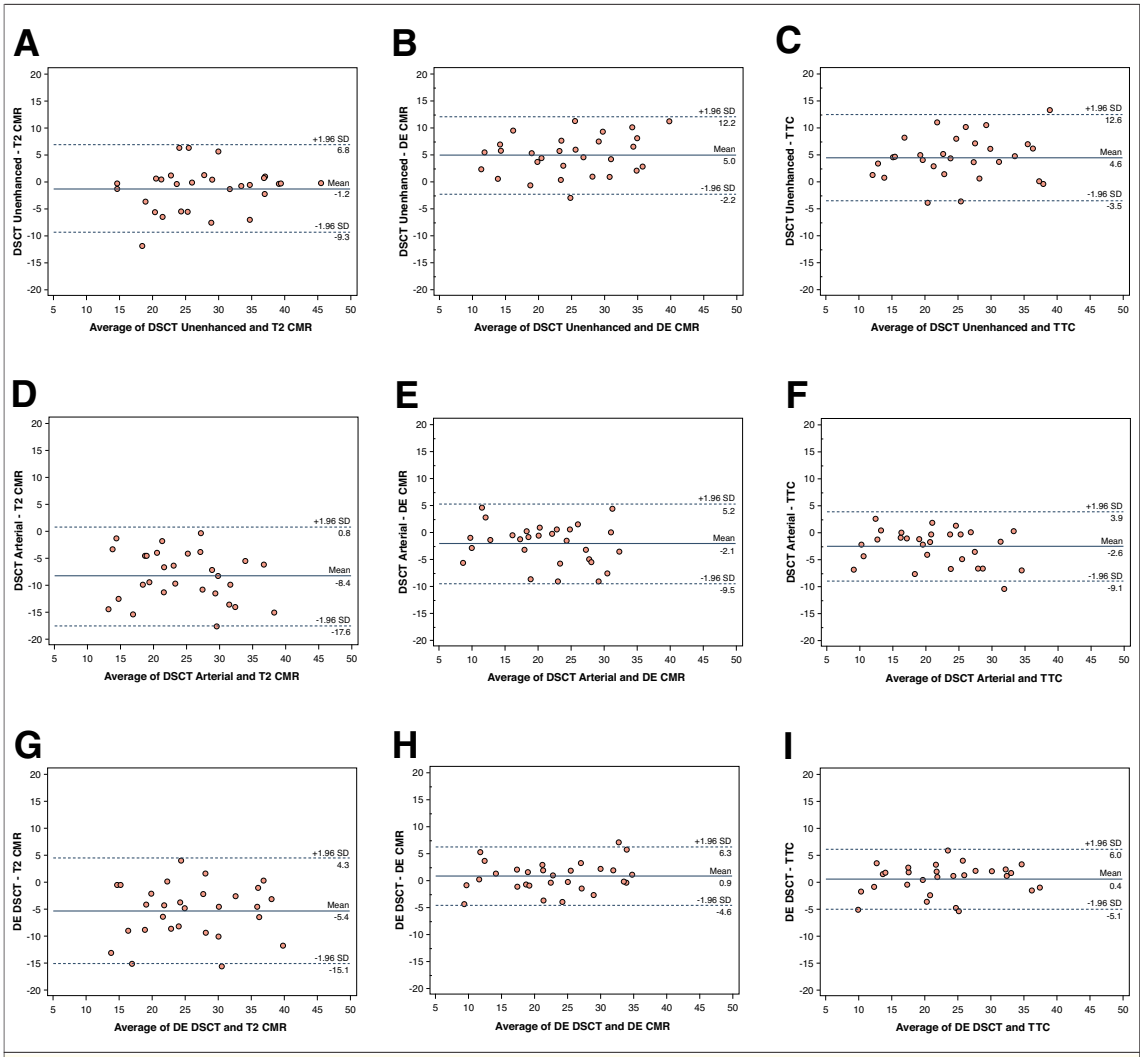

Figure 2. Agreement Between the Different Imaging Techniques

Bland-Altman plots compare myocardial infarction (MI) size as determined from **(A to C)** unenhanced, **(D to F)** arterial, and **(H, I)** late-phase dual-source computed tomography (DSCT) with **(A, D, G)** T2-weighted and **(B, E, H)** delayed enhanced (DE) cardiac magnetic resonance (CMR), as well as with **(C, F, I)** 2,3,5-triphenyltetrazolin-chloride (TTC) staining. **(H, I)** There is excellent agreement between DE DSCT and DE CMR and TTC. **(A)** The same is true for the comparison of unenhanced DSCT and T2-weighted CMR. The latter, however, presents with a potentially relevant scattering.

weighted CMR. However, these areas of edema are not to be confused with strongly hypodense areas on unenhanced CT scans as they were described in healed MI (20,22,23). The latter may even present with negative CT values and are thought to correspond to fatty infiltrations, which

Table 3. SNR and Attenuation Values as Determined From DSCT and CMR for Different Regions of Interest*

	DSCT						CMR	DE
	Unenhanced		Arterial Phase		Late Phase			
	Attenuation (HU)	SNR	Attenuation (HU)	SNR	Attenuation (HU)	SNR	T2 SNR	SNR
Infarction	28.4 ± 8.9	5.5 ± 1.9	45.3 ± 25.3	8.5 ± 6.5	131.3 ± 13.9	22.9 ± 6.1	102.6 ± 28.7	62.8 ± 11.7
Normal	53.8 ± 5.0	10.2 ± 0.9	90.7 ± 9.6	15.7 ± 5.6	74.8 ± 6.4	13.1 ± 3.7	53.1 ± 22.0	15.3 ± 6.6
LV cavity	38.7 ± 1.9	7.3 ± 0.5	439.8 ± 102.1	76.0 ± 31.4	114.6 ± 8.3	19.9 ± 4.4	66.3 ± 55.6	43.5 ± 19.7

*The SNR of CMR was markedly higher when compared with the different DSCT techniques.
HU = Hounsfield units; LV = left ventricular; SNR = signal-to-noise ratio: other abbreviations as in Table 1.

are known to occur in chronic MI. In contrast, myocardial edema occurs in acute MI and presents with CT values >0 HU.

Size of myocardial edema as determined from DSCT and T2-weighted CMR overestimated the true size of MI, as has been reported previously (3). The area presenting with edema, but without delayed contrast enhancement, has been suggested to correspond to the peri-infarction zone, which may benefit from revascularization (4). Considering the reported finding, CT may also permit for the differentiation of acute from chronic MI by assessing myocardial edema. This finding is relevant for clinical decision making. Although other indicators of MI such as wall motion abnormalities or wall thinning are assessable with cardiac CT (22), none of them unequivocally characterizes acute or chronic MI. Wall motion abnormalities are present in a reversible as well as in irreversible ischemic injury, whereas wall thinning does not necessarily occur in nontransmural MI.

Assessment of myocardial edema with DSCT faces some problems, however. The difference in the CT values is low, resulting in the need to apply high tube-current time products to keep the image noise in acceptable ranges and to provide an acceptable CNR. The unenhanced CT scan will therefore result in the same radiation exposure as a coronary CT angiogram. Using prospective ECG triggering and the most recent CT techniques, the dose may be reduced to ≈1 to 3 mSv (24), which is in the range of coronary calcium scoring, considered a screening technique. Unlike arterial and late-phase CT for assessing MI, there are no reference values for differentiating areas of edema from healthy myocardium. In this study, a difference of 12 HU was used to differentiate edema from healthy myocardium. This threshold was arbitrarily chosen by using twice the level of image noise as determined from the LV blood pool. Although this technique works in an animal setting, it has yet to be proven in patient studies.

Study limitations. Beyond these general problems with CT imaging of myocardial edema, there are some limitations that are specifically related to this study. First, all animals suffered from transmural MI. Thus, there is no information on the visualization of edema in subendocardial MI. Second, all examinations were performed in acute MI. To establish the use of this technique for differentiating acute from chronic MI, further studies of chronic MI are needed. Furthermore, interobserver and intraobserver variability were not assessed in this feasibility study. For quantifying MI size from late-phase CT, they are known to be in the range of 3% and 1%, respectively (25). Because of the poor CNR, they have to be considered higher in the CT assessment of myocardial edema. The development of dedicated post-processing techniques may facilitate the delineation of myocardial edema and thereby overcome this problem to some degree.

CONCLUSIONS

Unenhanced DSCT permits the detection of myocardial edema in acute MI. This technique can be combined with arterial and late-phase CT, potentially enhancing the diagnostic utility of cardiac CT as an imaging modality for a comprehensive workup of patients with suspected myocardial ischemia. Further studies confirming these findings in clinical examinations are needed.

Reprint requests and correspondence: Dr. Andreas H. Mahnken, Department of Diagnostic Radiology, University Hospital, RWTH Aachen University, Pauwelsstrasse 30, Aachen D-52070, Germany. *E-mail: mahnken@rad.rwth-aachen.de.*

REFERENCES

1. Abdel-Aty H, Zagrosek A, Schulz-Menger J, et al. Delayed enhancement and T2-weighted cardiovascular magnetic resonance imaging differentiate acute from chronic myocardial infarction. Circulation 2004;109:2411–6.
2. Stork A, Muellerleile K, Bansmann PM, et al. Value of T2-weighted, first-pass and delayed enhancement, and cine CMR to differentiate between acute and chronic myocardial infarction. Eur Radiol 2007;17:610–7.
3. Stork A, Lund GK, Muellerleile K, et al. Characterization of the peri-infarction zone using T2-weighted CMR and delayed-enhancement CMR in patients with acute myocardial infarction. Eur Radiol 2006;16:2350–7.
4. Dymarkowski S, Ni Y, Miao Y, et al. Value of t2-weighted magnetic resonance imaging early after myocardial infarction in dogs: comparison with bis-gadolinium-mesoporphyrin enhanced T1-weighted magnetic resonance imaging and functional data from cine magnetic resonance imaging. Invest Radiol 2002;37:77–85.
5. Buecker A, Katoh M, Krombach GA, et al. A feasibility study of contrast enhancement of acute myocardial infarction in multislice computed tomography: comparison with magnetic resonance imaging and gross morphology in pigs. Invest Radiol 2005; 40:700–4.
6. Mahnken AH, Koos R, Katoh M, et al. Assessment of myocardial viability in reperfused acute myocardial infarction using 16-slice computed tomography in comparison to magnetic resonance imaging. J Am Coll Cardiol 2005;45:2042–7.

7. Nieman K, Shapiro MD, Ferencik M, et al. Reperfused myocardial infarction: contrast-enhanced 64-section CT in comparison to MR imaging. Radiology 2008;247:49–56.
8. Habis M, Capderou A, Ghostine S, et al. Acute myocardial infarction early viability assessment by 64-slice computed tomography immediately after coronary angiography: comparison with low-dose dobutamine echocardiography. J Am Coll Cardiol 2007;49:1178–85.
9. George RT, Silva C, Cordeiro MA, et al. Multidetector computed tomography myocardial perfusion imaging during adenosine stress. J Am Coll Cardiol 2006;48:153–60.
10. Nikolaou K, Sanz J, Poon M, et al. Assessment of myocardial perfusion and viability from routine contrast-enhanced 16-detector-row computed tomography of the heart: preliminary results. Eur Radiol 2005;15:864–71.
11. Hoffmann U, Millea R, Enzweiler C, et al. Acute myocardial infarction: contrast-enhanced multi-detector row CT in a porcine model. Radiology 2004;231:697–701.
12. Skiöldebrand CG, Lipton MJ, Redington RW, Berninger WH, Wallace A, Carlsson E. Myocardial infarction in dogs, demonstrated by non-enhanced computed tomography. Acta Radiol Diagn (Stockholm) 1981;22:1–8.
13. Ter-Pogossian MM, Weiss ES, Coleman RE, Sobel BE. Computed tomography of the heart. AJR Am J Roentgenol 1976;127:79–90.
14. Adams DF, Hessel SJ, Judy PF, Stein JA, Abrams HL. Computed tomography of the normal and infarcted myocardium. AJR Am J Roentgenol 1976; 126:786–91.
15. Georgiou D, Bleiweis M, Brundage BH. Conventional and ultrafast computed tomography in the detection of viable versus infarcted myocardium. Am J Card Imaging 1992;6:228–36.
16. Cury RC, Nieman K, Shapiro MD, et al. Comprehensive assessment of myocardial perfusion defects, regional wall motion, and left ventricular function by using 64-section multidetector CT. Radiology 2008;248:466–75.
17. Lardo AC, Cordeiro MA, Silva C, et al. Contrast-enhanced multidetector computed tomography viability imaging after myocardial infarction: characterization of myocyte death, microvascular obstruction, and chronic scar. Circulation 2006;113:394–404.
18. Gerber BL, Belge B, Legros GJ, et al. Characterization of acute and chronic myocardial infarcts by multidetector computed tomography: comparison with contrast-enhanced magnetic resonance. Circulation 2006;113:823–33.
19. Park JM, Choe YH, Chang S, et al. Usefulness of multidetector-row CT in the evaluation of reperfused myocardial infarction in a rabbit model. Korean J Radiol 2004;5:19–24.
20. Sanz J, Weeks D, Nikolaou K, et al. Detection of healed myocardial infarction with multidetector-row computed tomography and comparison with cardiac magnetic resonance delayed hyperenhancement. Am J Cardiol 2006;98:149–55.
21. Mahnken AH, Bruners P, Kinzel S, et al. Late-phase MSCT in the different stages of myocardial infarction: animal experiments. Eur Radiol 2007;17: 2310–7.
22. Winer-Muram HT, Tann M, Aisen AM, Ford L, Jennings SG, Bretz R. Computed tomography demonstration of lipomatous metaplasia of the left ventricle following myocardial infarction. J Comput Assist Tomogr 2004;28:455–8.
23. Zafar HM, Litt HI, Torigian DA. CT imaging features and frequency of left ventricular myocardial fat in patients with CT findings of chronic left ventricular myocardial infarction. Clin Radiol 2008;63:256–62.
24. Petersilka M, Bruder H, Krauss B, Stierstorfer K, Flohr TG. Technical principles of dual source CT. Eur J Radiol 2008;68:362–8.
25. Baks T, Cademartiri F, Moelker AD, et al. Multislice computed tomography and magnetic resonance imaging for the assessment of reperfused acute myocardial infarction. J Am Coll Cardiol 2006;48:144–52.

Key Words: myocardial infarction ■ computed tomography ■ cardiac magnetic resonance.